Robotic Inspection by Database Matching

Henry Thorne, F. B. Prinz, and H. 0. K. Kirchner

CMU-Rl-TR-85-4

Department of Mechanical Engineering
The Robotics Institute
Carnegie-Mellon University
Pittsburgh, Pennsylvania 15213

March 1985

Current address for H. O. K. Kirchner: Department of Solid State Physics, University of Vienna, A-1090 Boltzmanngasse 5, AUSTRIA.

Table of Contents

List of Figures

ABSTRACT

We have developed a method of inspection which does not require reference points or accurate fixturing. This inspection system reports world coordinate positions of points along the edge of a part. Where these points lie on the part is unknown, except that they are on the edge, and they form a space curve which is similar to the ideal part described by a Computer Aided Design database. The two point sets are, however, referenced to different coordinate systems and contain points at different positions along the curve. First, corresponding points are formed between the databases by using the coordinate independent measures of perimeter length and curvature. The coordinate transform between the two databases is then determined by singular value decomposition. Finally, a comparison of the two databases determines out-of-tolerance points.

1 INTRODUCTION

The object of this paper is to introduce a method of part location and shape inspection. This requires the comparison of a standard piece with a test piece to determine congruency of shape. Once the latter is found to be reasonably congruent to the former, the displacement between the two, a combination of rotation and translation, can be found. Obviously, if the congruency is insufficient, no reasonable definition of the translation and rotation that are supposed to produce congruency is possible.

Currently, automated shape inspection systems use a set of gauging points, or surfaces, to first locate the part, then to inspect it. A gauging point is a point whose x,y,z position is known in all relevant coordinate systems, a gauging plane is the planar equivalent. Suggested in this paper is an alternate method where the location and inspection of the part are performed simultaneously, without the use of gauging points. Two databases are assumed, one being a description of the shape of the ideal part (the ideal CAD database) and the other being a description found by a robotic inspection system (the inspector database). By matching these databases, the transform between the two coordinate systems can be obtained without having to utilize gauging points.

If each database contains a list of points describing a space curve (e.g., an edge), then the difficulty with performing the task is that the ideal database points do not correspond to the inspector database points. In general, an inspection system which records the position of discrete points will not contain the position of the same points found in the ideal database, but points somewhere between them. Thus, one cannot simply find the transform between matching points (a relatively slmple task).

A strategy to accomplish this task is developed for surfaces with edges. Comparing the ideal database with the inspector database can be defined and accomplished independently of any coordinate system by using scalar geometric invariants. This is particularly feasible for space curves. Although surfaces have geometrically invariant properties, the invariants are not necessarily scalar and are not as easily accessible. In principle, however, the strategy proposed can be extended to surfaces without edges, i.e., egg-shaped or geoid shaped parts.

Once the part description has been reduced to the behavior of scalar invariants along the space curve, the problem is reduced to finding the phase shift of a scalar signal between the standard and the test piece. Human/optical recognition prefers

points of infinite curvature, i.e., corners (Attneave 1954), whereas we try to find the phase shift from a Fourier fit along the parameter (Brill 1968; Zahn and Roskies 1972). Unlike the authors quoted and cognitive scientists in general (Pavlidis 1977, 1978; Kovalevsky 1980), we do not stress optical recognition, but our emphasis is to extract quantitative data on congruency and location in a manufacturing environment.

The strategy is in line with recent developments of pattern recognition where topological (Pavel 1983), or field theoretical (Machuca and Phillips 1983) methods are used. In particular, the idea of using geometric invariants has been proposed before (Kasvand and Otsu 1982; Wallace, Mitchell and Fukunaga 1981).

2 DIFFERENTIAL GEOMETRY

Suppose we have a space curve, say the front edge of the hood in an automobile. Its location *in* space is given by the coordinates z(x) and y(x). This would have to be compared with the coordinates of the standard piece $\hat{z}(x)$ and $\hat{y}(x)$. An examination of congruency would then require the homogeneous transformation by rotation R and translation T of our. set of vectors x(x,y,z) into another set of vectors $\hat{x}(x,y,z)$ so that

$$R\,x + T \rightarrow \hat{x} \tag{2.1}$$

Alternatively, the space curve could be described by the dependence of the three space coordinates on one scalar parameter, say the arc length s

$$x(s)\quad y(s>\quad z(s), \tag{Z2}$$

but this still requires a comparison according to (2.1). We try to profit from the fact that the concept of congruency is coordinate independent. According to differential geometry (Laugwitz 1960; Struik 1961), the change of the vector x with components *K* y and z with ds is the unit tangent vector t

$$\underset{\sim}{t} = d\underset{\sim}{x}/ds \tag{23}$$

Since the tangent can be thought of as the limit of the secant, the tangent passes through two consecutive points on the curve. One can find the osculating plane through three consecutive points on the curve, and then draw a circle through these. The radius *p* of this osculating circle is related to the change of the tangent vector along the curve by

$$\frac{1}{P}\underset{\sim}{n} = *\underset{\sim}{n} = d\underset{\sim}{t}/ds = d^2\underset{\sim}{t}/ds^2 \qquad (2.4)$$

where K is called curvature and the unit vector n is called the principle normal. The center c of the osculating circle to x lies at

$$\underset{\sim}{c} = \underset{\sim}{x} + p\underset{\sim}{n} \qquad (2.5)$$

The principle normal $\underset{\sim}{n}$ and the tangent vectors $\underset{\sim}{t}$, are normal to each other. Since the former lies in the osculating plane, the cross product of the tangent vector and the normal is itself the normal of the osculating plane, called the binormal (see Fig. 1)

$$\underset{\sim}{b} = \underset{\sim}{t} \times \underset{\sim}{n} \qquad (2.6)$$

For non-planar, or twisted curves, $\underset{\sim}{b}$ changes along the curve and

$$d\underset{\sim}{b}/ds = - r\underset{\sim}{n} \qquad (2.7)$$

where r is called the torsion. Together with a third equation that can be easily derived, (2.4) and (2.7) are the formulae of Serret-Frenet

$$\begin{aligned} 6tJ6s &= *\underset{\sim}{n} \\ d\underset{\sim}{n}/ds &= - */ + r\underset{\sim}{b} \\ d\underset{\sim}{b}/ds &= - r\underset{\sim}{n} \end{aligned} \qquad (2.8)$$

The basic theorem of differential geometry states that the two functions

$$*\{s) \text{ and } r(s) \qquad (2,9)$$

define a space curve. Any two curves which can be described by the functions (2.9) are said to be congruent though they may be displaced by a rotation and translation with respect to each other. We benefit from this by measuring K and r along the edges of automotive parts and judge their congruency according to this criterion.

Any combination or function of * and r is another invariant and can be used to describe the curve. Following the geometric representation of the above, one can ask for the sphere that goes through four consecutive points of the curve, the osculating sphere. The center $\underset{\sim}{d}$ of the osculating sphere to $\underset{\sim}{x}$ Is uniquely determined by

$$\mathbf{d} = \mathbf{x} + /\!>\!\mathbf{n} + r\left(\frac{dp}{ds}\right) \mathbf{b} \qquad (2.10)$$

where

$$R^2 = p^2 + r^2 \left\{\frac{dp}{ds}\right)^2 \qquad (2.11)$$

is the square of radius of the osculating sphere.

Consider a point $\underset{\sim}{x}$ on the curve. The following Taylor expansion, in terms of the arc length, follows from Frenet's formulae

$$\begin{aligned} Cx(AS) - x(0)l_1 &= AS\frac{2}{6}AS^3 \\ Ex(AS) - xft»]_n &= \frac{\kappa}{2} AS^2 \quad \frac{d}{6} AS^3 \qquad (2.12) \\ CXCASJ - x(0\}]^\wedge_b &= \frac{\kappa\tau}{6} AS^3 \end{aligned}$$

This can be used to find the linear and **quadratic apprpximAtion** to **the** arc length between two points x_n and x_{n+1} on the curve.

$$L^2 = (x_{n+1} - x_n)^2 = \Delta S^2 - \frac{\kappa^2}{12}(\Delta S)^4 + \ldots \qquad (2.13)$$

or, Inverted,

$$AS \bullet L \qquad \{2.14\}$$

in the **linear,** and

$$AS \approx \bullet\!\!-\!\!\bullet \quad 1 - \quad \mathbf{1} - \frac{\mathbf{2, 2}}{3} \qquad 12.151$$

in the quadratic **approxtmatioa**

In numerical work, the use of equations (2.4) and (2.7) requires numerical differentiation if *K* and r are to be found. The alternative is to find *K* and another invariant, the radius of the osculating circle, by constructing the circle through three points, and constructing the sphere through four consecutive points, respectively. This geometric approach uses (2.5) and (2.10) and avoids numerical differentiation.

3 GEOMETRIC INVARIANTS

The new data needed for evaluation can be obtained by tactile scanning or by laser scanning. It is not necessary to obtain coordinates along the edges of a part, coordinates along any prominent feature line should be sufficient- To illustrate the strategy proposed, we assume that the x coordinates of a set of N unequally spaced points

$$P_n \qquad n = 1,...,N \tag{3.1}$$

have been measured along a space curve. A circle is constructed through each triplet $P_{\cdot}, P, P_{\_}$, and the radii are attributed to P , as shown in Fig. 2. In a similar way, spheres are constructed through the quadruples $P_{\cdot}, P, P_{\_\_}, P_{o}$, and their radii are assigned to P_n. This provides a listing of the two following sets of invariants.

$$p(x) \text{ and } R(x) \qquad n = 1,...,N \tag{3.2}$$

The next task is to compute the arc lengths between P_{n-1} and P_n, either in the linear or quadratic approximation, equations (2.13) and (2.14), respectively. These are added to obtain the invariant descrrptions

$$p_n(S_n) \text{ and } R_n(S_n) \qquad n = 1 \text{ W } N \tag{3.3}$$

where

$$S = \sum_{i=0}^{n} AS. \tag{3.4}$$

It should be noticed that the complete description of the part in question has been reduced to the dependence of two scalar functions.

4 FINDING THE PHASE SHIFT BETWEEN THE IDEAL DATABASE AND THE INSPECTOR DATABASE

4.1 A FOURIER METHOD

Once the strategy of finding the invariant descriptions

$$p(s) \quad \text{and} \quad R(s) \tag{4-1}$$

has been executed for the test curve, it remains to be seen if they can be made congruent to the invariant descriptions

$$\hat{p}(s) \quad \text{and} \quad \hat{R}(s) \tag{4.2}$$

of the standard piece. The examination of congruency no longer requires a homogeneous transformation of vectors x on the test piece into vector $\hat{x}$ on the standard piece, because by now it has been reduced to finding an optimum scalar shift s_o so that

$$R(s + s_o) \rightarrow \hat{R}(s) \tag{4.3}$$

If the data on the standard piece *(4.2)* are essentially given in form of pfecewise continuous functions, finding a shift scalar s_o to fulfill (4.3) is merely a least square fit problem.

More Interesting and difficult is the case where both data, basts (4.1) and (4.2) are in the form of points spaced at irregular Intervals, One possibility is to interpolate one set by splines and fit the other set to this spline In principle the s_o obtained does depend on the spline shown. This drawback can be avoided by using a Fourier transform technique. By some rough matching, for example by examination of the ranges of $p, \hat{p}$ R and $\hat{R}$ a common interval for all four *Mtw* sets is chosen. On this support of length t, Fourier series are computed, which Is possible even for oddly spaced points, This gives

$$p(s) \approx \sum_{k=0}^{M} A_k \sin 2\pi f_c \frac{k}{L} + B_k \cos 2\pi k \frac{k}{L} \tag{4.4}$$

and

$$R(s) = \sum_{k=0}^{M} C_k \sin 2\pi k \frac{s}{L} + D_k \cos 2\pi k \frac{s}{L} \qquad (4.5)$$

where at most $M \leq N/2$ coefficients are computed. Similar fits are found for $\hat{I}(s)$ and $\hat{R}(s)$ with coefficients $\hat{A}_k$, $\hat{B}_k$, $\hat{C}_k$ and $\hat{D}_k$. The task of finding a suitable shift s_o so that (4.3) is fulfilled, becomes, in terms of the Fourier coefficients

$$A_k \sin 2\pi k \frac{(s + s_o)}{L} + B_k \cos 2\pi k \frac{(s + s_o)}{L}$$

$$= \hat{A}_k \sin 2\pi k \frac{s}{L} + \hat{B}_k \cos 2\pi k \frac{s}{L} \qquad (4.6)$$

Combining with identities:

$$\sin(a + b) = \sin(a)\cos(b) + \cos(a)\sin(b)$$

$$\cos(a + b) = \cos(a)\cos(b) - \sin(a)\sin(b)$$

results in the matrix expression

$$\begin{pmatrix} \cos 2\pi k \frac{s}{L} & -\sin 2\pi k \frac{s}{L} \\ \sin 2\pi k \frac{s}{L} & \cos 2\pi k \frac{s}{L} \end{pmatrix} \begin{pmatrix} A_k \\ B_k \end{pmatrix} = \begin{pmatrix} \hat{A}_k \\ \hat{B}_k \end{pmatrix} \qquad (4.7)$$

for all k. In the two dimensional $A_k B$ plane one has to find a phase angle $2\pi k s_o/L = C$ so that a rotation by the angle ζ being denoted by $R(\zeta)$,

$$R^k(\zeta) \begin{pmatrix} A_k \\ B_k \end{pmatrix} = \begin{pmatrix} \hat{A}_k \\ \hat{B}_k \end{pmatrix} \qquad (4.8)$$

for all k, or

$$2\pi k s_o/L = kC \pm \arctg(\hat{B}_k/\hat{A}_k) - \arctg(B_k/A_k, \quad \mod 2\pi) \qquad (4.9)$$

This provides M values of s_o for each of the two invariants. Ideally they should all be the same, but this will not be the case in practice.

4.2 A HILL-CLIMBING METHOD

if the curves are similar in shape, there should be a shift of one (periodic) curve which would align it with the other such that there would be nearly zero area between them. Thus, another method of determining the shift between the two, periodic curvature versus length plots, is that of minimizing the area between the two curves with respect to trial shifts. The area between the two curves for a postulated shift x is computed then the areas for (x + *) and (x - *) are computed. One of the three areas will be smaller than the other two. If it is the postulated shift, x, then a smaller perturbation * is tried and the two areas are calculated again. However, if it is one of the perturbed shifts, then this becomes the postulated one and the procedure starts again. This can be carried out until the perturbation becomes small enough that an accuracy limit is reached.

This method has several problems associated with it. Notably, local minimal areas which do not represent the true shift may be found (the wrong hill may be climbed). Hence, this method should only be used once a good starting guess is achieved that will not lead to the wrong minimum. It is, however, very powerful for getting very accurate curve matching when a good initial guess is used.

5 LOCATION

Once the shift between the ideal and the inspector data is found, there are different strategies possible for the location. At this stage, s values on the test piece and $\hat{s}$ values on the standard piece have been correlated up to an offset of s_o. This reduces the location of the part to the identification of a number of points P_m on the test piece with corresponding points on the standard piece. Even though the measured points on both the standard and the test piece will not correspond to each other, corresponding points can be obtained either by interpolation or by repeated measurement. All that remains to be done is to find the rotation R and the translation T so that

$$R\underline{x} + T \rightarrow \hat{\underline{x}}$$

for these N points. The minimization of the square distance between $(R\underline{x} + T)$ and $\hat{\underline{x}}$ for ail N points requires minimization of

$$\ell(R,T) = \sum_{k=1}^{N} \langle\, Rx^k + T - \hat{x}^k \mid Rx^k + T - J^k \,\rangle \tag{5.1}$$

with respect to R and $\underline{x}$, the superscript k is the summation index. The "bra-ket" notation $\langle \underline{a} \mid \underline{b} \rangle$ is used for the inner product of two vectors $\underline{a}$ and $\underline{b}$. Minimization with respect to T is achieved from

$$\partial\ell/\partial T = \sum_{k=1}^{N} \langle\, \underline{T} \mid Rx^k + \underline{T} - \hat{x}^k \,\rangle = 0 \tag{5.2}$$

with the solution

$$N \langle\, T \mid = - R \sum_{k=1}^{N} \langle\, h \mid + \sum_{k=1}^{N} \langle\, x^k \mid \tag{5.3}$$

With the center of gravity coordinates

$$N^{-1} \sum_{k=1}^{N} \langle\, x^k \mid = y \tag{5.4}$$

$$N^{-1} \sum_{k=1}^{N} \langle\, x^k \mid = \hat{y} \tag{5.5}$$

the shift T is merely the shift between the centers of gravity

$$\langle\, T \mid = - Ry + \hat{y} \tag{5.6}$$

and with new coordinates counted from the center of gravity

$$x^k - y = t \tag{5.7}$$

$$\hat{x}^k - \hat{y} - f \tag{5.8}$$

there remains only an equation for minimization with respect to R:

$$\text{fiRi} - \sum_{k=1}^{N} X^{-1} \langle\, Rh - 7 \mid Rh - 5 \,\rangle \quad \text{is 9)}$$

Since R is orthogonal

$$\langle\, R^{\wedge} \mid Rf \,\rangle - \langle\, 4 \mid U \,\rangle \tag{5.10}$$

and (5.9) is equivalent to maximizing

$$g(R) = \sum_{k=1}^{N} \left\langle R\zeta^k \mid \zeta^k \right\rangle = \left(\sum_{k=1}^{N} \zeta^k \zeta_j^k \right) R_{ij} \tag{5.11}$$

in index notation, with sums over i and j. If the bracket is diagonalized by a singular value decomposition with orthogonal matrices U and V,

$$g(R) = U_{ts} U_{js} \left(\sum_{k=1}^{N} Z \; W \right) V_{i\ell} V_{n\ell} R_{nt} = D_{s\ell} O_{\ell s} \tag{5.12}$$

where

$$D_{s\ell} = U_{js} \left(\sum_{k=1}^{N} Z \; W \right) V_{JL} \tag{5.13}$$

is diagonal and

$$O_p = V \bar{} R \bar{U} \tag{5.14}$$

is orthogonal so that

$$O \; O = i \tag{5.15}$$

The last condition can be multiplied by a Lagrangian matrix

$$0 = (O \; O - 6) L_P \tag{5.16}$$

and finally the function

$$h(R) = g(R) + 0 = 0\,(0 + O_{ns} O_{nt} L_{tl} - L_{s\pounds}) \tag{5.17}$$

has to be made an extremum. Differentiation with respect to L gives

$$0 = 3h/3L = D\,fO\,0\,2\,5_P - D\,\#5\,3. \tag{5.18}$$

which Is solved by

$$0 * 1 \tag{5.19}$$

Differentiation of (5.17) with respect to O gives

$$0 = 3h/3O \; ^{\wedge} \; D \; A \; s \; \& \; p \; ^{\wedge} \; \& \; S \; O \; L. * 0 \; i \; a \; L \; . \; 1 \tag{5.20}$$

which, with {5.19} has the solution

(5.21)

1

The solution (5.19) can be inserted into (5.14) to find the original rotation:

$$R_{ij} = v_{is} u_{js} \qquad <5\text{-}22>$$

A different derivation of this result can be found in Hanson and Norris (1981).

6 EXAMPLES

In the following two sections, the methods described above are performed for an ideal space curve, an oblong ellipse, and for a realistic sample from the automotive industry, an automobile hood.

6.1 OBLONG ELLIPSE

The egg shaped curve shown in Figure 3:

$$y = \cos(\text{theta})$$

$$x = 10 \times \sin(\text{theta}) \qquad 0° \leq \text{theta} < 180°$$

$$x = 2 \times \sin(\text{theta}) \qquad 180° \leq \text{theta} < \mathbf{360°}$$

was chosen because it is closed and not periodic in curvature (as an ellipse would be). Ninety points were distributed at even intervals in theta (theta = Q, 4, 8,_,356) thus creating a series of line segments of unequal length to form a CAD database for the ideal space curve.

Each point was assigned a radius of curvature by fitting a circle through it and its two adjacent points. Curvature was assigned to each point by inverting the radius of the circle described above. Each point was also assigned a delta length which was the distance between the previous point and itself, using the Euclidean norm. Length was assigned as the sum of the delta lengths from s = 0 to the given point. Each point thus had a position (x,y), radius of curvature, curvature, delta length, and length associated with it. From this data, the curvature can be plotted as a function of length. This is also shown in Figure 3.

If a robot or other automated inspection system were to **measure the** position of

points along the space curve, a similar database could be formed. It wou however, have three major differences. One, some error (noise) would be introduc in the measurement of position- Two, the points measured by the inspector wot not correspond to the points of the Ideal database. It for example, the edge of ruler were the space curve in question, the ideal database might give the positions the Inch marks while the inspector might find the positions of every other half in mark. Thus the number of points the inspector might find would most likely i different from the number of points in the ideal database. And third, the point whi< the ideal data-base considers to be the beginning of the database Is most likely n going to be the point the robot inspector first finds. Thus, the point at s • 0 In or database might not be anywhere near the point where s * 0 in the other database.

In order to simuJat* a database produced by the robot inspector, the Ideal databas wee copied into the 'snsptctor database and the following three operations performec

1, Fluctuation (see F?gyr# 4); Each point was randomly moved along the space curva, using linear interpolation between the points, within a window dtsignattd *fi&duMion** The window was normalized to the length of the nearest point Thus if lite fluctuation window were 0,5, a point coyftl be movtd halfway to the nearest point If random chance so elected™ Pfttctyatfon was kept between 0.0 and 0,49 for simulation purposes since points could overlap when fluctuation was 0.5.

2* Motse .*see Figure 5lc Each point *WB$* movtcJ to a random location within a box of width, designated *noi$$$* in the two dimensions Ix and y}« This differs from fluctuation in that the movement Is not restricted along the space curve. The box size was normalized to the distance to the nearest *pnmt* Simulating the accuracy of measurement systems (where accuracy Is proportional to volume}. Thus rf noise were set to 1%, and the nearest point were 10 cm away, the point would b# randomly r«iocat«d in a box 1 *mm mi$%' m* * and 1 *mm* witf© in y_f centered about the point's original position.

3* $hrft i'ssi? :? gn*e C? The pb;nr con'$idtrtd to be the beginning of the iptcs *z&)te i% * ^ mz%* altered to th« one n#*r#sl a given valy« *$Mft* Tn£f Ajts ro e?*ec! *cr* tft psstt.fon of the points, but ctusts only a shift **in the curvature plot.**

The p-sfo*'ft'tt l\$ *lrnr* ?o Mt€f^r-rt8 A^nere in Iha ideal database woyld the first point *I'm* mta5^.*fTt*r* *s-ji*:** & ^o^ra- ?M$ stuff *m $,* between the ideal databaaa **and** *tn§* f^p^r^t ^3?*£3^e. *s:on'2* a¥ci^ *u$* to form corresponding points *to¥* **linear** ^te^po$ *T* r«r/.««e^ ^» *^tstz^t^* D^^!$ to the ideal points. Once corresponding »'<jcrt» ... r{(f ... *d*irg tn# coordinati ir«niform between the **two databases is greatly reduced.**

To find the shift, both the Fourier coefficient method and the minimized area between the curves method were used. First, the median value of the first ten shifts produced by the Fourier coefficient method was used on the radius of curvature plot {inverse of curvature). Note that clipping the value of the length of the total curve was used to avoid near infinite values at straight line sections. The shift reported here was accurate to within one percent of the total length. The hill-climbing method of Section 4.2 was then used to achieve higher accuracy, and for the example shown with 10% noise (unreasonably high), and 0.5 fluctuation, an accuracy of 0.0081% of the total length was found for the shift shown. Figure 7 shows the plot of the shifted results on top of the ideal data.

With this shift, translation and rotation between the ideal and inspector database is determined by the methods described in Section 5 (Location). After performing their transformation, the accuracy of the process is determined by calculating the shortest distance from each inspector database point to the closest line segment on the inspector database.

One hundred and sixty trials were run to determine the average accuracy of the algorithm. Four values of *fluctuation* were tried against four values for *noise,* with *ten* trial shifts for each combination. The resulting accuracy is shown in Table 1. The curve was 25.156 units long, and for 1% noise with 0.3 fluctuation (much worse than the measurements will hopefully be) the average error was 0.0033 units. To determine the effectiveness of this strategy in an actual manufacturing environment, the simulation of the next example will produce error measurements in millimeters.

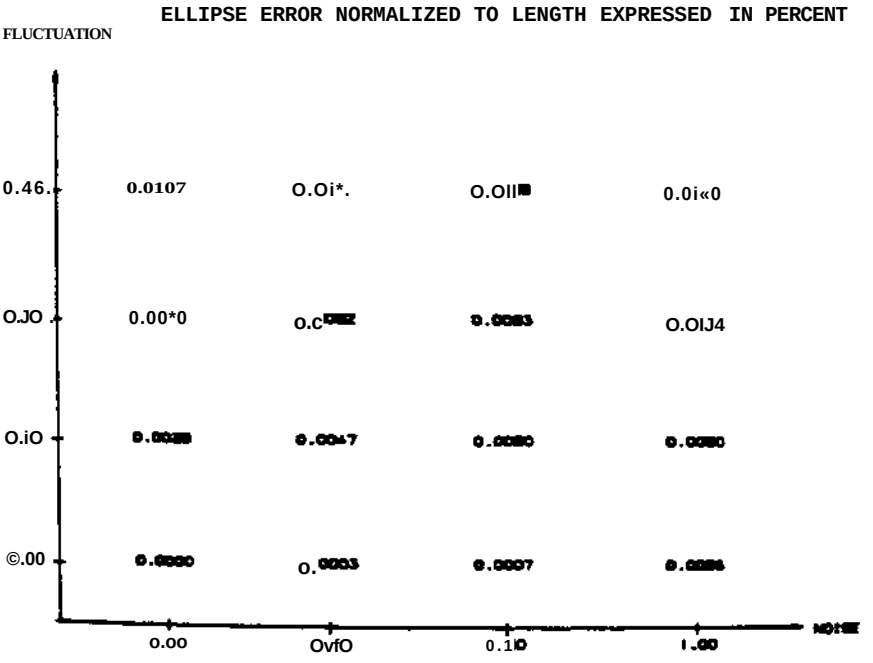

Table 1: Ellipse error based on ten trials for each parameter pair.

6.2 AUTOMOBILE HOO©

A CAD database of an automotive hood was obtained as shown in Figure 8. The perimeter lines were extracted to form the ideal database for the space curve of the edge. The 5.719 meter long edge was described by the three dimensional coordinates of 218 points around the edge with concentration of points roughly proportional to curvature.

Once again, curvature and length were assigned to each point and plotted as shown in Figure 9. A mock inspector database was also formed by taking each ideal point and fluctuating it adding noise, and shifting the s « 0 point (as described in the previous **example).** The resulting curvature plot is shown in Figure 10.

As In the previous **example,** 160 trials were run to **determine** the average error for different values of *fluctuation* and *noise** The results (see Table 2) are surprisingly good, especially considering the second derivative nature of curvature. For high values of noise and fluctuation {1% and 0.5), the error is one-fifth of a millimeter. This Is well within the tolerances used by the automotive industry during hood inspection of piys or minus **one-half** a millimeter along the critical edges.

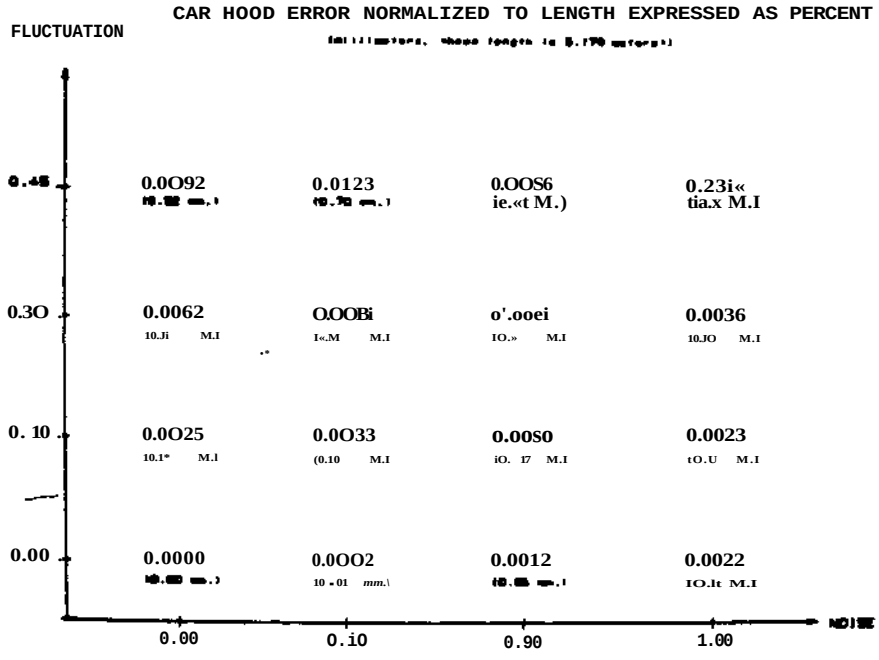

Table 2: Average automobile hood error over ten trials for each parameter pair.

REFERENCES

1. Attneave, F. 1954. Some Informational Aspects of Visual Perception. *Psycho!. Rev.* 61(3): 183-193.

2. Brill, E. L. 1968. *Character Recognition via Fourier Descriptions,* Wescon, Paper 25/3, Los Angeles.

3. Hanson, R. J., and Norris, M. J. 1981. Analysis of Measurements Based on the Singular Value Decomposition. *SJ.A.M. J. Sci. Stat. Comput.* 2(3): 363-373.

4. Kasvand, T., and Otsu, N. 1982. Regularization of Piecewise Linear Digitized Plane Curves for Shape Analysis and Smooth Reconstruction. *Proc. 6th Int. Coni'.Pattern Recognition,* vol. 1. Silver Spring: IEEE Computer Society Press, 468-471.

5. Kovalevsky, V. A. 1980. *Image Pattern Recognition.* New York: Springer,

6. Laugwitz, D. 1960. *Differentialgeometrie.* Stuttgart: Teubner.

7. Machuca, R., and Phillips, K. 1983. Application of Vector Fields to image Processing. *IEEE Trans. Pattern Analysis Machine Intelligence* PAMt-5{3>:316-329.

8. Pavel, M. 1983. The Impact of Categorical and Shape Theoretical Formalisms upon Pattern Recognition. *Proc. 6th int. Conf. Pattern Recognition,* vol. 2. Sliver Spring: IEEE Computer Society Press, 638-640.

9. Pavlidis, T. 1977. *Structural Pattern Recognition.* Berlin: Springer, 147.

10. Pavlidis, T, 1978. Algorithm for Shape Analysis of Contours and Waveforms. *Proc. 4th Int. Joint Conf. Pattern Recognition.* Long Beach: IEEE Computer Society, 70-85.

11. Struik, D. J. 1961. *Differential Geometry.* London: Addison-Wesley.

12. Wallace, T. P., Mitchell, 0. R., and Fukunaga. 1981. Three Dimensional Shape Analysis Using Local Shape Descriptors. *IEEE Trans. Pattern Analysis and Machine Intelligence* PAMI-3(3k310-323.

13. Zahn, C. T., and Roskies, R. Z. 1972. *Fourier Descriptors for Plane Closed Curves.* IEEE Trans. Comp. C-21(3}:269-281.

Figures

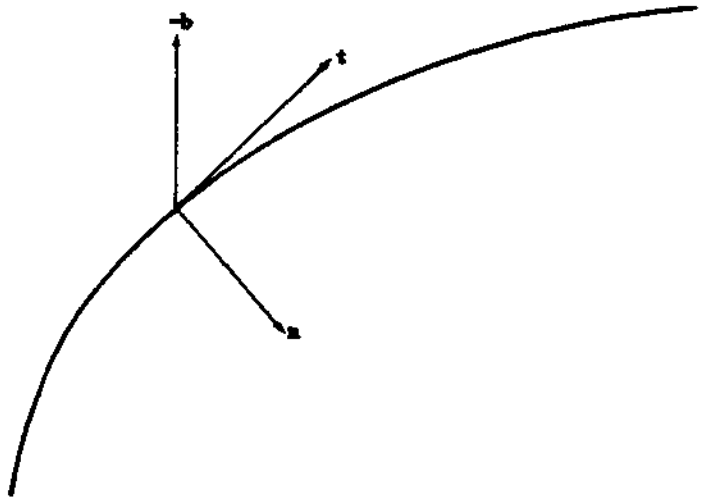

Figure 1: The tangent vector $\bar{t}$ and the normal vector $\bar{n}$ lie in the osculating plane with normal $\bar{b}$.

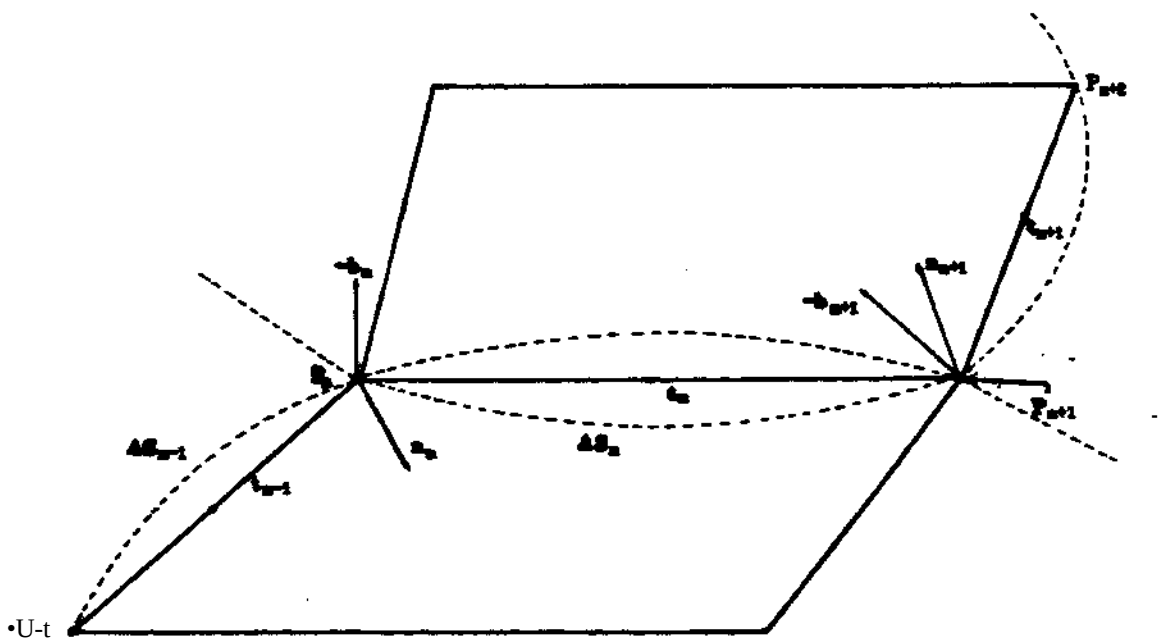

Figure 2: The three consecutive points P_{n-1}, P_n and P_{n+1} lie in the osculating plane with normal $\vec{n}$. Within these 3 points the osculating circle with radius p_n is constructed.

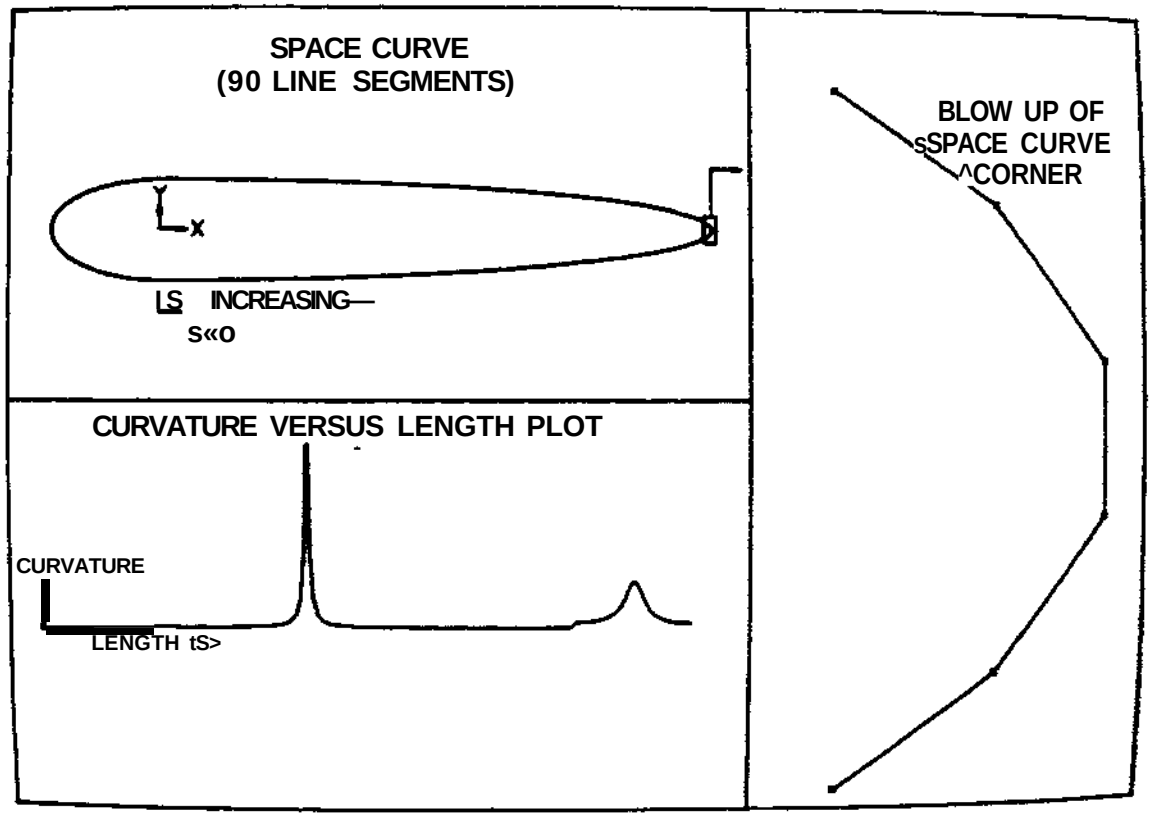

Figure 3: Ideal database for obtong ellipse.

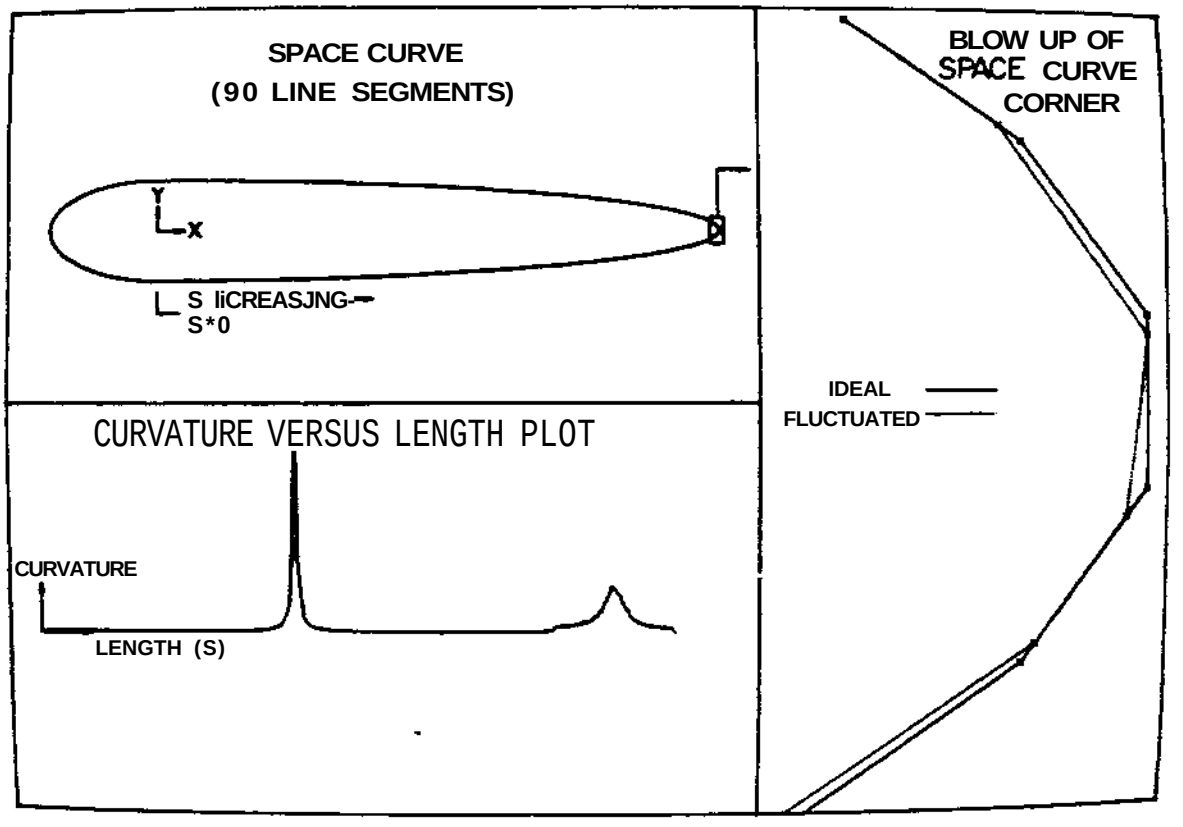

FSgy r© 4: After fluctuating the points (0.5 "fluctuation") of the ideal database.

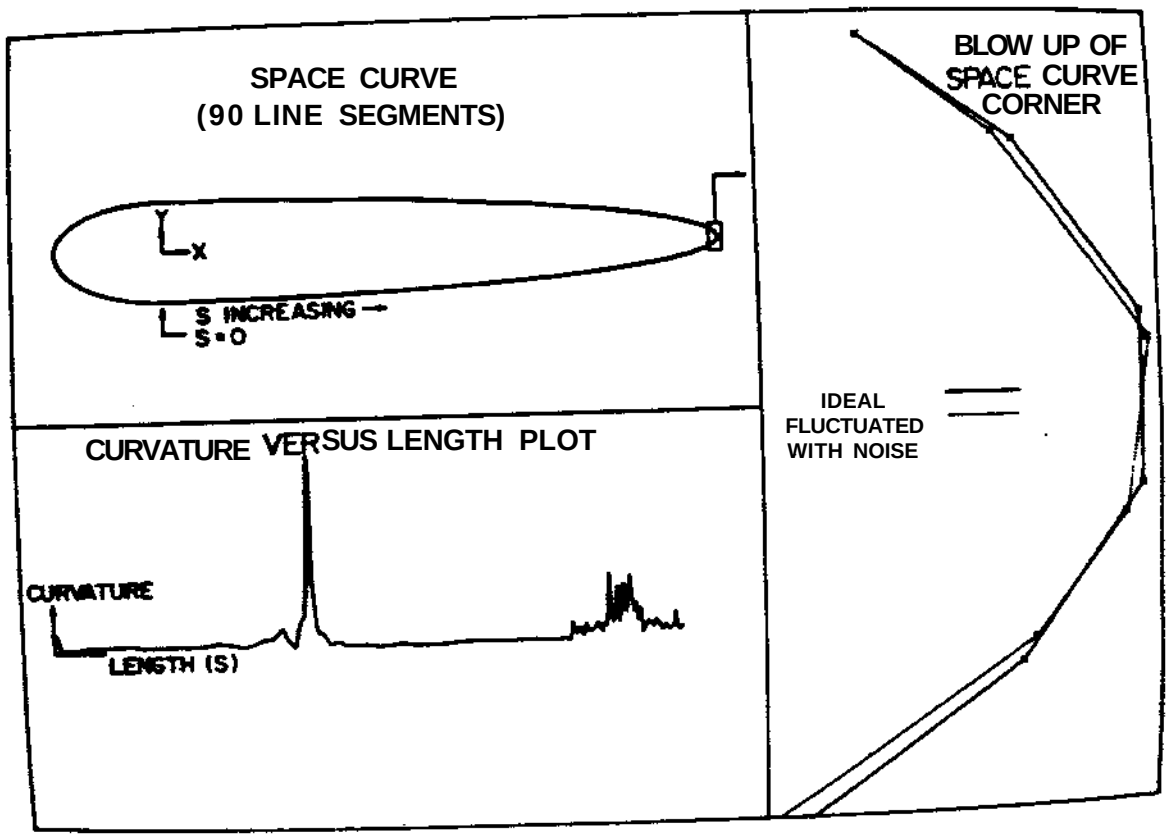

Figure 5: After adding noise (10%) to the fluctuated database.

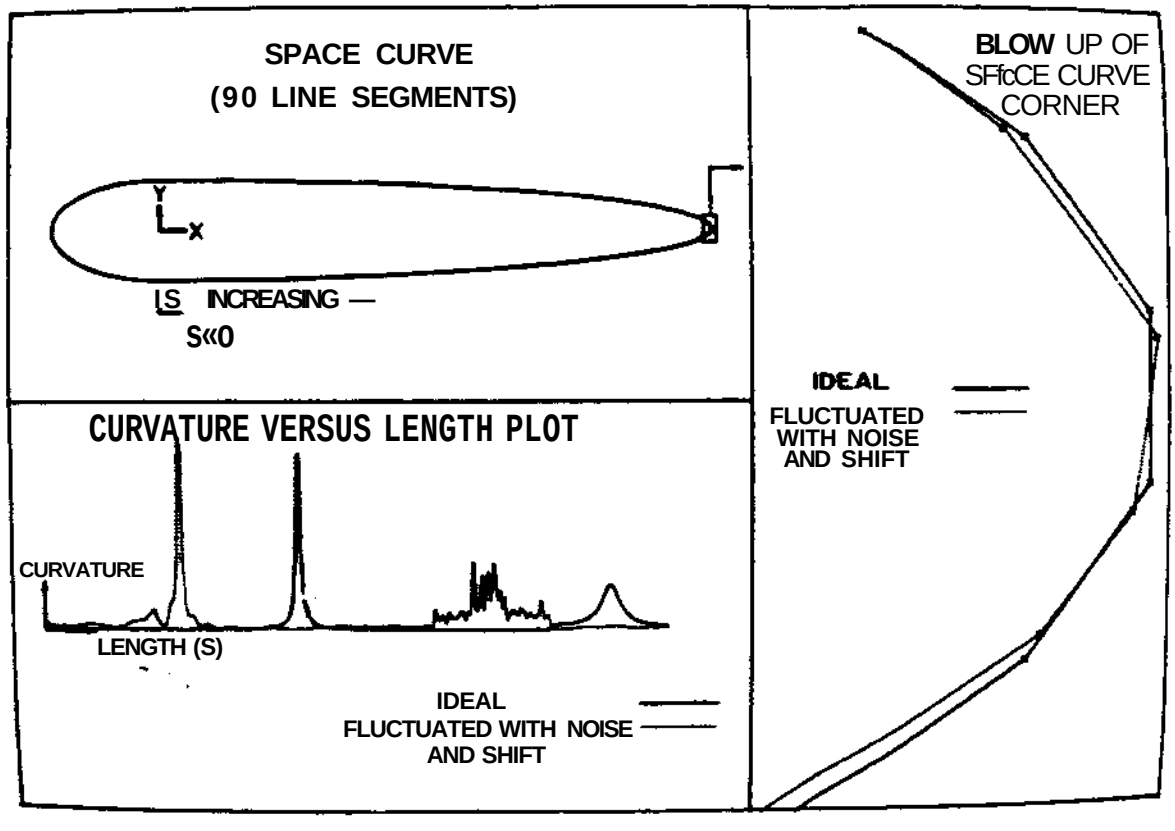

Figu re 6: After shifting the noisy, fluctuated database.

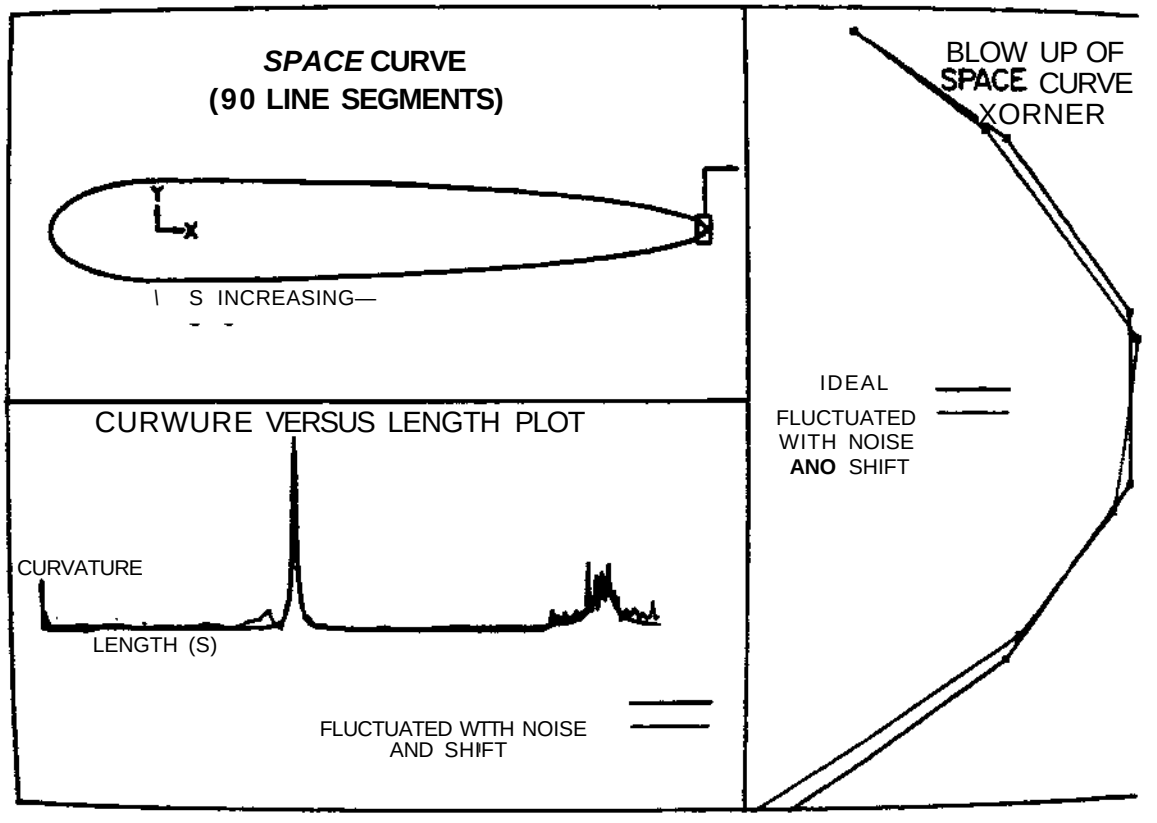

FIgu re 7: The best fit of the inspection database to the ideal database.

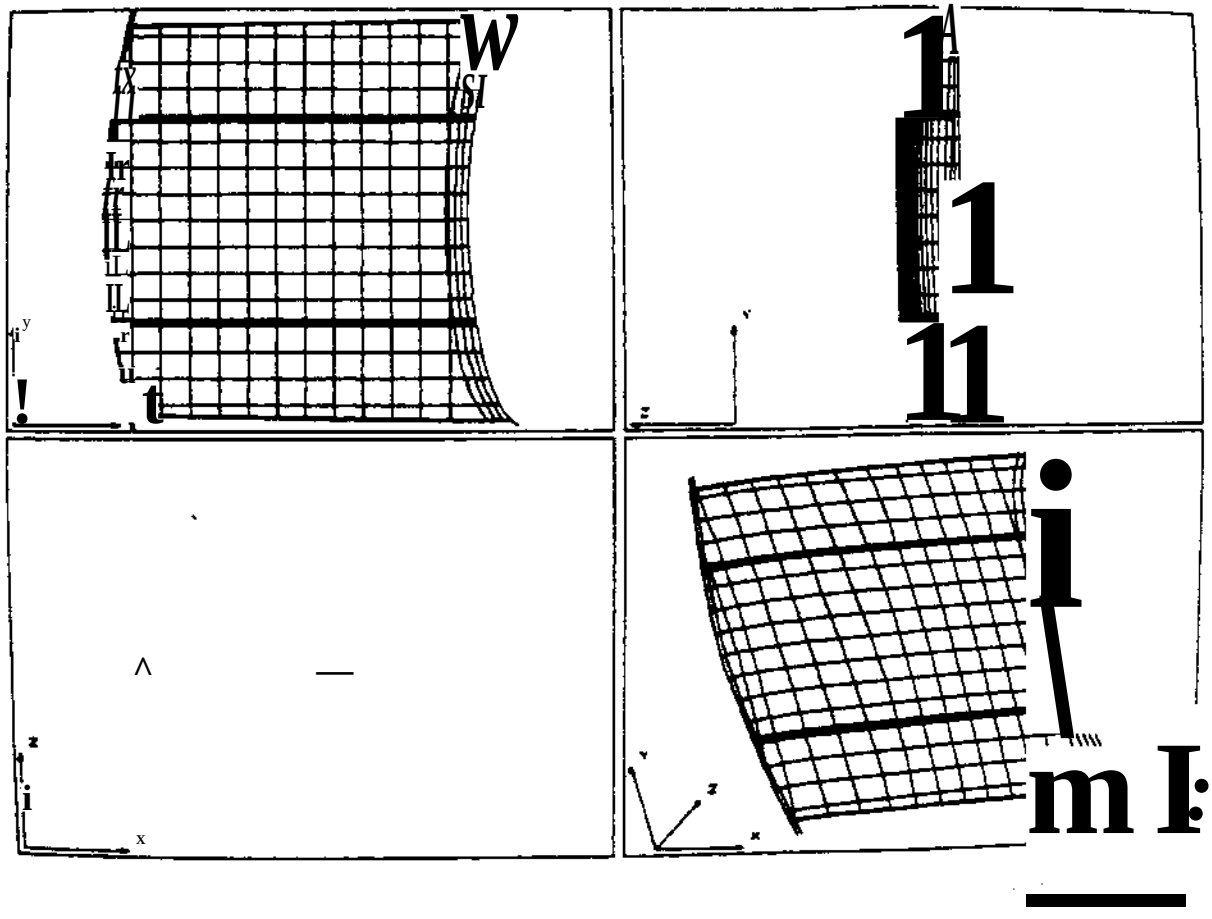

Figu re 8: CAD database for automobile hood.

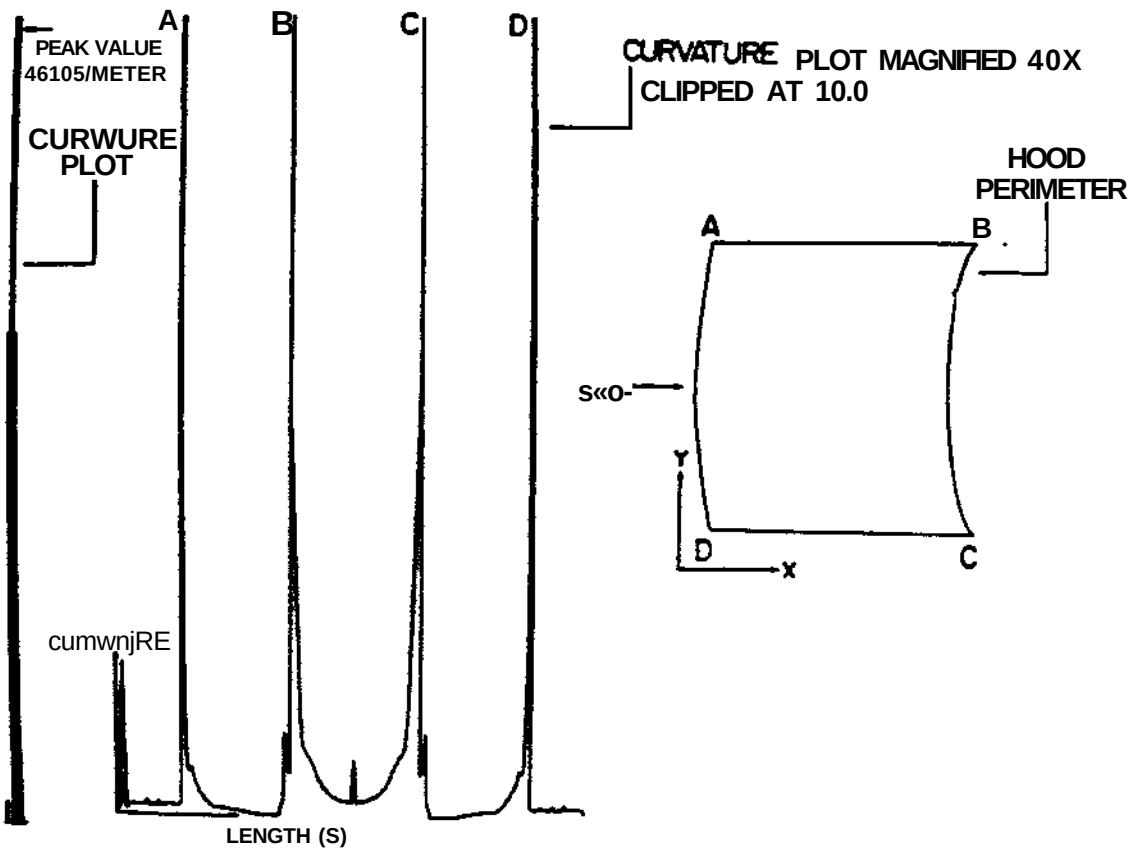

Figure 9: Curvature plot for ideal hood database.

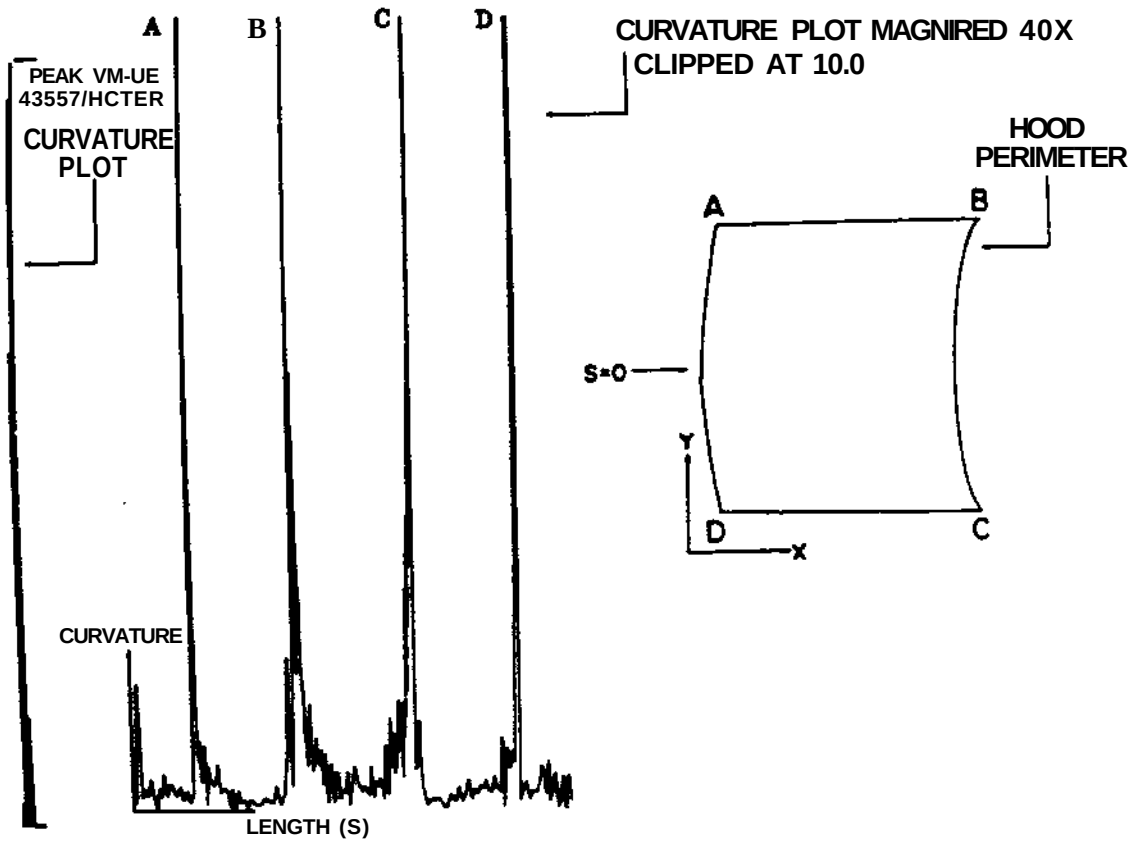

Figure 10: Curvature plot for inspection database.